Multiphysics modelling of Titanium alloy Ti-6Al-4V realised by Wire Arc Additive Manufacturing (WAAM)

Alizée Remy, Matthieu Rauch, Jean Yves Hascoet, Guillaume Rückert

Multiphysics modelling of Wire Arc Additive Manufacturing (WAAM) for Titanium alloy Ti-6Al-4V

Alizée Remy[a,b], Matthieu Rauch[a,b],

Jean-Yves Hascoët[a,b], Guillaume Ruckert[b,c]

(a) Nantes Université, École Centrale Nantes, CNRS, GeM, UMR6183, F-44000 Nantes, France

(b) Additive Manufacturing Group, Joint Laboratory of Marine Technology (JLMT) Centrale Nantes – Naval Group, France

(c) Naval Group - DT/ MET/CESMAN - Technocampus Ocean 5 rue de l'Halbrane 44340 Bouguenais

Mails: alizee.remy@ec-nantes.fr ; matthieu.rauch@ec-nantes.fr ; jean-yves.hascoet@ec-nantes.fr ; guillaume.ruckert@naval-group.com

Ti-6Al-4V alloy is particularly interesting in the Naval industry due to its good mechanical properties, low density and corrosion resistance. Additive manufacturing causes changes in material properties on macroscopic, mesoscopic, and microscopic scales. Current research focuses on the process modelling of WAAM on such a scale. However, there exists a limited number of studies focusing on on Ti-6Al-4V with a realistic heat source model. In this work, the characteristics of Ti-6Al-4V beads and walls were realised with the Cold Metal Transfer (CMT) WAAM. Considering fluid mechanics, and thermal physics during material phase changes, a realistic multi-physics model was built using the Volume of Fluid (VOF) approach. Additionally, two CMT transfer modes were modelled with the different implementations of the power signal, standard and pulse. Ultimately, the results were validated experimentally. The method not only predicted the beads and walls' dimensions but also anticipated their shape and topology according to the material characteristics. Moreover, this methodology brought remarkable results as it proved that the heat source was close to the electric arc. Finally, the experimental data confirmed the importance of the numerical analysis on the process efficiency. Future works will focus on predicting microstructural changes in titanium alloys based on thermal data.

Keywords: Wire Arc Additive manufacturing, Ti-6Al-4V alloy, Cold Metal Transfer, Thermofluid model, The volume of Fluid method.

1 Introduction and state of the art

1.1 *Additive manufacturing and WAAM process generalities*

Additive Manufacturing processes (AM) have been evolving continuously within the industry for several years. These technologies involve adding material, layer by layer, to minimize material wastage, (Singh, 2021), (Wu, 2018).

Additive manufacturing can employ a wide range of materials. Metallic materials play a significant role in many industries, particularly in application fields such as aeronautics, aerospace, medical, and, naval, (Shah, 2023), (Rauch, 2022), (Rauch, 2021). Indeed, these methods often offer numerous advantages compared to traditional manufacturing processes such as casting, and forging. The metal AM processes can reduce the cost of parts and production times. They also allow the production of more complex parts while maintaining good mechanical properties.

This study focuses on one particular AM process, Wire Arc Additive Manufacturing (WAAM). WAAM is based on the DED (Direct Energy Deposition) principle, while using wire as feedstock material and an electrical arc as heat input (Shah, 2023). The process boasts a high material flow rate, enabling the rapid manufacture of large and complex parts, (Shah, 2023). (Figure 1) provides a schematic representation of the process (Xin, 2021).

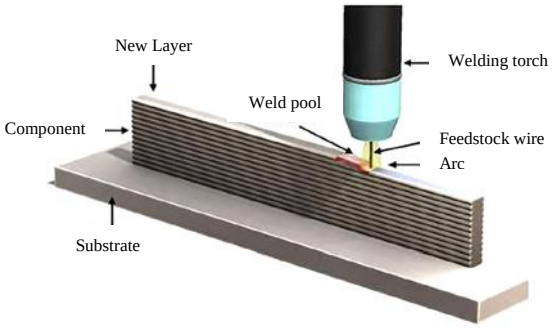

Figure 1: Schematics of the WAAM system principle (Xin, 2021)

The figure demonstrates the layer-by-layer material deposition on the substrate. The wire is fed into the arc and then, thanks to an electric pulse. Once the layer is deposited, the torch stops. The objective of this idle time is for the previously added bead to cool down and obtain a solid state. Then the newly formed layer is applied and the procedure repeats. One particular challenge of working with metals is to avoid oxidation. Thus, current solutions have introduced shielding gases in the process. Such an example is presented in this study, the metal-inert Gas process, also known as Gas Metal Arc Welding (GMAW).

1.2 *CMT and CMT+P transfer modes*

GMAW works with several transfer modes, Cold Metal Transfer Technology (CMT) and Cold Metal Transfer Technology Pulse (CMT+P). CMT is a modified GMAW process, that involves the control of current and wire movement during the short circuit transition (Srinivasan, 2022), (Prado-Cerqueiria, 2017). The novelty of this method is it superimposes an electrical and mechanical pulse in a synchronized manner (Benoit, 2018). Throughout the short-circuit phases, the power supply is cut off and the retraction movement of the wire is regulated. The retraction is a significant motion as it determines the droplet formation. As a result, the process produces less spatter and demands reduced heat input, (Fronius, 2023). CMT+P is a blend of CMT and pulsed arc. In this mode, an additional drop is deposited with each cycle, increasing the deposition rate. The characteristic curves for CMT Pulse cycle is presented in (Figure 2). There are two pulses in this chart, them take place in between CMT.

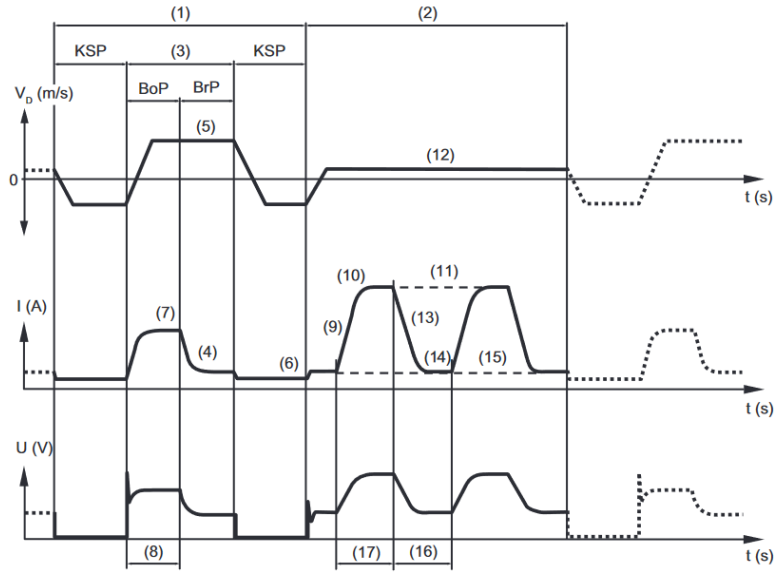

Figure 2: Wire speed rate, current and voltage curves during a CMT Pulse cycle. KSP = short-circuit phase, BoP = power ramping phase, BrP = burning phase, (1) CMT phase, (2) Pulse phases, (3) Plasma phase, (Fronius, 2021)

However, one encounters many challenges GMAW such as part poor accuracy, deformations, and cracks due to residual thermal stresses. The first mentioned can be a result of the process capabilities, while deformations and cracks occur due to the high or low cooling rates that produce abnormal thermal gradients in the part (Justus, 2022), (Montevecchi, 2016). These phenomena have an impact on the micro, meso, and macroscale of the part. Therefore, current research focuses on the application of numerical simulation for studying the properties at macro, meso, and microscopic scales.

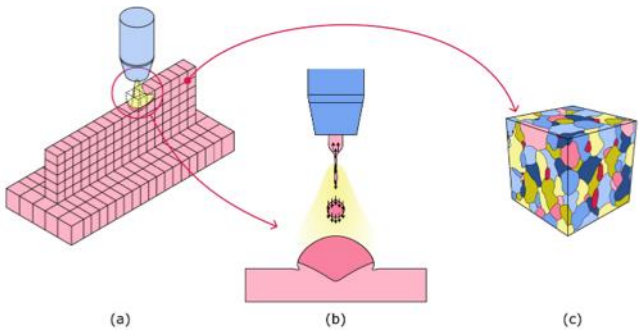

Figure 3: Three scales to modelise WAAM process : (a) macroscopic, (b) mesoscopic (c) microscopic, (Sampaio, 2023)

(Figure 3a)) illustrates the deposition of layers, while (Figure 3b)) presents the layer fusion at the same time but on a mesoscopic scale. Similarly, (Figure 3c)) provides a microscopic view of an infinitesimal element. However, the development of multi-scale models is challenging due to their complexity. Therefore, studies are concentrating only on single scale numerical models.

One particular aspect studied from a macroscopic perspective is the thermal history to analyze and predict possible deformations or residual stresses. For example, Gokhale et al. developed a TIG-WAAM process model to analyze the effects of thermal cycles during manufacturing, (Gokhale, 2021). Similarly, Montevecchi et al. created a thermomechanical study that identified and optimized the process parameters, (Montevecchi, 2016). While their research improved the process, it was unable to describe the heat transfer in the arc and its formation (Sampaio, 2023), (J. Goldak, 1984). On the contrary, mesoscale models allow describing these phenomena and predicting their impact on the material properties. For many years researchers have been interested in thermo-fluid model. For instance (Hamid, 1989), developed a predictive model for weld pool. Numerical approaches such as the VOF (Volume Of Fluid) method are adapted to establish thermo-fluid models for welding (Panwisawas, 2018), and AM, (Cheon, 2016). This multi-physics approach considers four different material states and their interactions (plasma, gas, liquid and solid). It is particularly suitable for problems involving highly deformed free surfaces. This method is capable of tracking the free surface of droplets and the molten pool. Such models offer a more realistic representation of the thermal physics of the WAAM heat source. For example, Cadiou et al. modelled the heat transfer and dynamics of the droplet in 2D (Cadiou, 2020). This model can predict the flow velocity and the temperature field during the deposition. 3D models are also established to study fluid movements of the melt in the three directions of space, (Cadiou, 2020), (Bai, 2018), (Zhao, 2023). In general, macro and mesoscopic multiphysics models can now be used to predict geometric, kinetic and thermal phenomena during the WAAM process. Additionally, the values of thermal gradients and cooling rates of the meso and macroscopic simulations are used in microscopic models. However, the data transfer from one to another is not as simple and it might result in non-accurate models. Thus, one must consider different numerical analyses for each scale.

To conclude, several thermo-fluid models of WAAM are proposed in the literature. Some are focusing on the droplet formation dynamics in 2D, others are interested in the

dynamics of the melt pool, while third ones are reviewing the thermal history of multi-layer deposits (Bai, 2018), (Zhao, 2023). Nevertheless, to the best of our knowledge, no model can be configured and distinguished from CMT and CMT+P. Therefore, this article focuses on integrating the two transfer models into a thermo-fluid numerical simulation. The objective is to predict the geometry and the surface topology of one bead and multi-layer wall using Ti-6Al-4V with the variation of process parameters.

2 Physics involved and hypotheses

Establishing a thermofluid model necessitates adherence to fundamental principles of physics. In the CMT process, the physical phenomena of the arc play a substantial role in influencing the flow and thermal distribution during deposition at the cathode, anode, and plasma. (Figure 4a)) outlines these phenomena, highlighting interactions among solids, liquids and gases. Meanwhile (Figure 4b)) delves into interactions between anode/plasma and cathode/plasma.

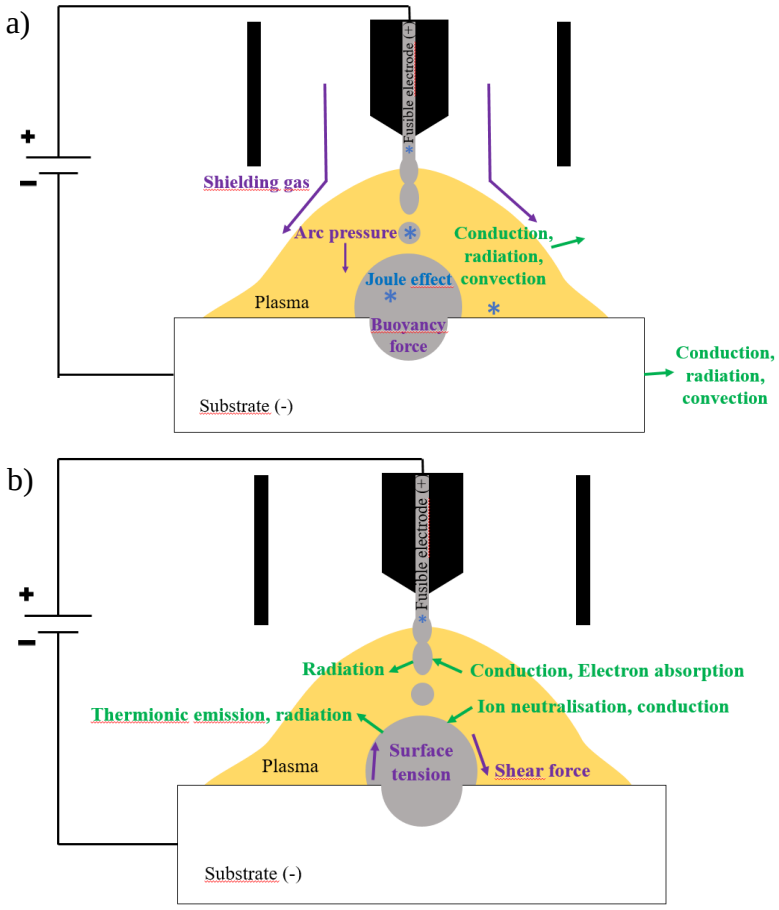

Figure 4: Main physical phenomena occurring during a MIG process. a) Solid, liquid and gas phases b) Anode/plasma and cathode/plasma interfaces, inspired by (Cadiou, 2020)

The phenomena described in the diagrams above are based on three different types of physics: fluid mechanics, thermal phenomenon and phase change. In order for one to model the problem, one must postulate some assumptions:

1. The shrinkage dynamics of the wire and droplets will not be taken into account.

2. The fluid flow of the gas phase and metal phase is incompressible, immiscible, laminar, and Newtonian in the whole domain.
3. The arc plasma is in local thermodynamic equilibrium (LTE), which means that the average temperatures of each particle species (ions, electrons and atoms) are the same throughout the arc plasma. In addition, the electron transfer enthalpy that occurs in the arc column is neglected as its effect is very small compared to Joule heating, (Cadiou, 2020).
4. Arc plasma follows a Gaussian heat distribution.
5. The electromagnetic effects of the arc (Lorentz forces) are negligible compared to other forces like surface tension, and arc pressure, (Cadiou, 2020).
6. The wire and heat source are perfectly coaxial.

Boundary conditions were applied on all the faces of the outer block that vary depending on the side of the block (Table 1).

Table 1: Boundary conditions system

Boundary	*Energy*	*Momentum*
All outer block faces except Zmax,	$T = 293K$	$\vec{V} = \vec{0}$
Zmax outer block, specified pressure	$T = 293K$	$P \cdot \vec{n} = P_{atm} \cdot \vec{n}$
Inner block faces except Zmax,	ΔT	$\vec{V} = \vec{0}$
Zmax inner block, specified pressure	$T = 293K$	$P = P_{atm}$
Heat source	ΔT	$V = TS$
Momentum source	ΔT	$V = TS$
Flow rate	ΔT	$V = WFS$
Shield Gas	ΔT	$P = P_{arc}$

Where T is the temperature, $\vec{V}$ is the velocity, P is the pressure, TS is the Travel Speed and WFS is the Wire Feed Speed. Following this theoretical groundwork, the model is prepared to provide the results as close to reality as possible.The previous assumptions were then used to design the computational domain. (Figure 5) presents a volume with dimensions 50mm × 25mm × 20mm.

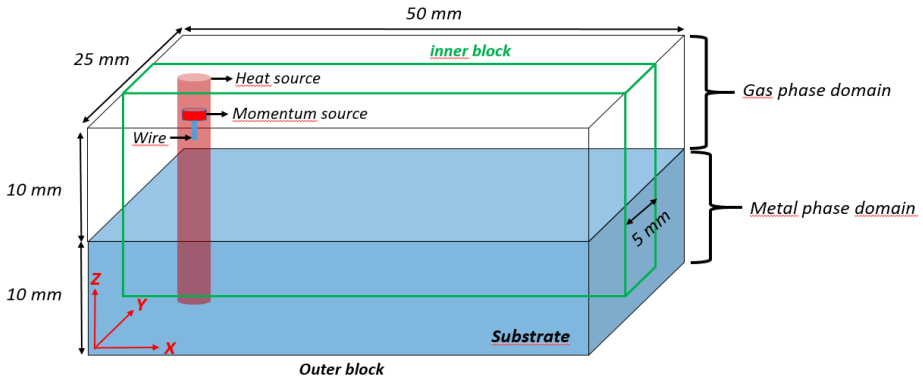

Figure 5: Schematic of the computational domain

This working volume is divided into several zones, the upper one filled with shielding gas and the lower one that represents the metal region. To optimize the computing time, the domain is discretised into non-uniform cubic blocks. The inner is placed in the middle and demonstrates the area of interest. Additionally, the sub-domain contains fine mesh with 5mm cells size and for providing a more realistic overview of the temperature gradient and velocity. The second block surrounds the inner one with coarse mesh. The wire feed is represented by a momentum source and is coaxial with the heat source. These two components are constitutive components of the torch and must move simultaneously. In the end, the time step was chosen to be 10^{-5}s for obtaining precise model.

3 Experimental and simulation methods

3.1 Experimental setup

The Cold Metal Transfer (CMT) technology from Fronius was used as shown in (Figure 6). A 6-axis anthropomorphic robot with a welding torch is used. The substrate used is a Ti-6Al-4V alloy with a size of 143mm *25mm *10mm. To work with this material, argon (99%) is used as inerting gas supplemented by a shielding gas consisting of 50% Ar + 50% He mixture at a flow rate of 17 L/min are essential to prevent oxidation.

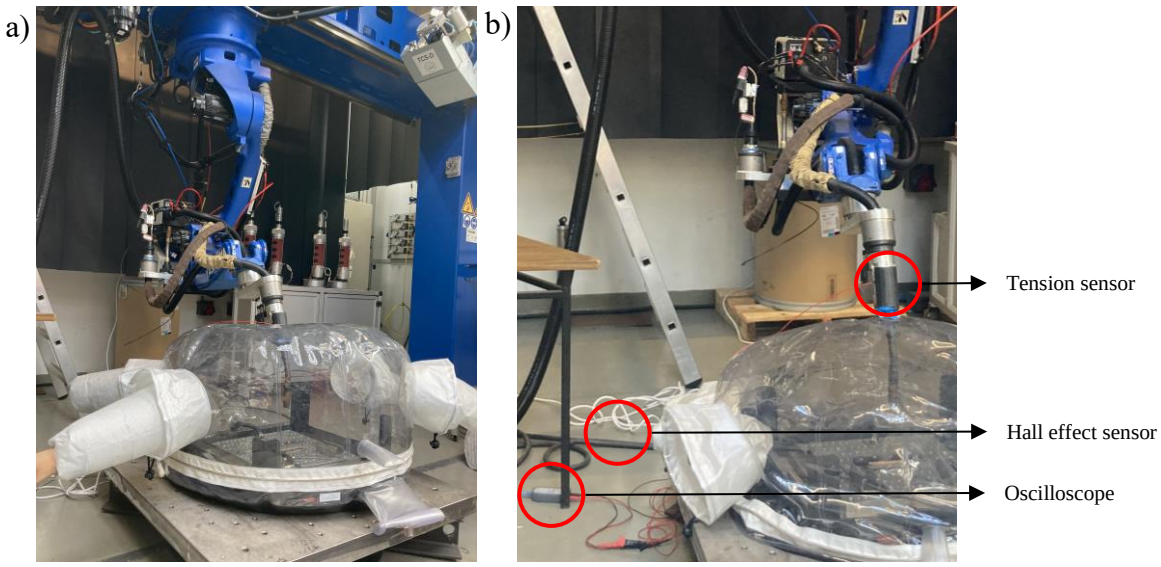

Figure 6: Experimental system

Table 2 : Process parameters with CMT (1-4) and CMT+P (5-8)

	CMT				CMT+P			
N°	1	2	3	4	5	6	7	8
TS (mm/min)	320	240	400	300	320	240	400	300
WFS (m/min)	8.0	6.0	6.0	6.0	8.0	6.0	6.0	6.0
WFS/TS	25	15	15	20	25	15	15	20

In this process, TS and WFS play a significant role in shaping the beads and walls' geometry. A range of variations in these parameters has been defined and tested for both CMT and CMT + P, as outlined in (Table 2). A ten-layer wall was manufactured using the single-layer parameters, with a TS of 300 mm/min and a WFS of 8 m/min. These

samples will serve as references throughout the study, as the process parameters will be utilized for model calibration.

An electrical monitoring system was established to capture the electrical signals, as illustrated in (Figure 7), during the experiments. The signals were analyzed to compute the arc powers corresponding to the various tests conducted. The calculated power values were 2000W and 1400W for samples 1 and 2, and 3500W and 2500W for samples 5 and 6. Notably, the power reduces as the wire feed parameter decreases. Additionally, a power reduction is observed for the CMT +P transfer mode compared to the CMT.

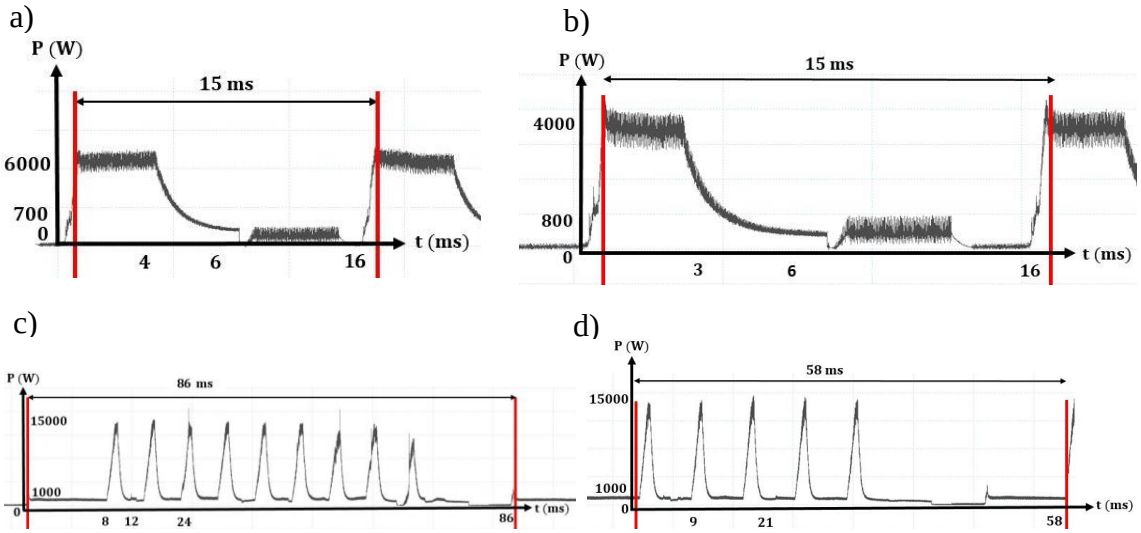

Figure 7: Electrical power, a) b) CMT, sample 1 and 2 c) d) CMT+ P, sample 5 and 6

Moreover, a schematic representation of the CMT power signal was presented in (Figure 8). This graph is based on approximated values of one 15ms period presented in (Figure 7a)). The estimated model was then integrated in the simulation set up and run periodically.

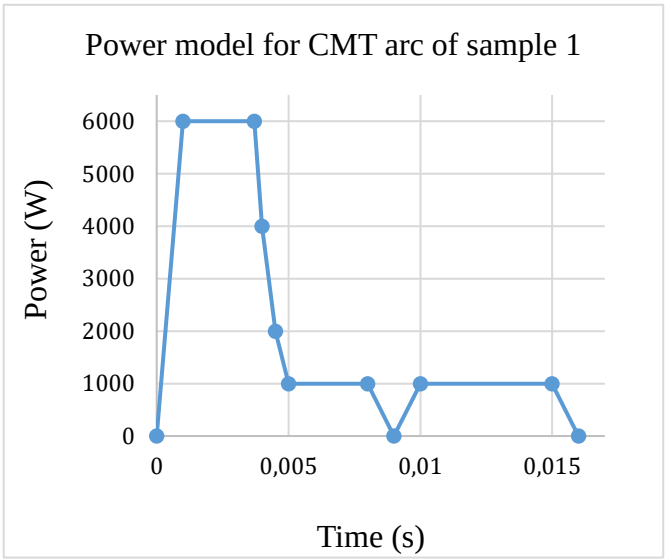

Figure 8: Power model of arc in CMT process as a function of time

In general, studies show that efficiency of WAAM process is effected by the dissipated arc energy due to thermal radiation, conduction and convection and material energy absorptivity (denotated as "K1" and "K2" in (Figure 9) respectively), (Cadiou, 2020). To precisely consider potential energy dissipation during deposition, an efficiency coefficient, "*K*" was calculated using the (Eq 1).

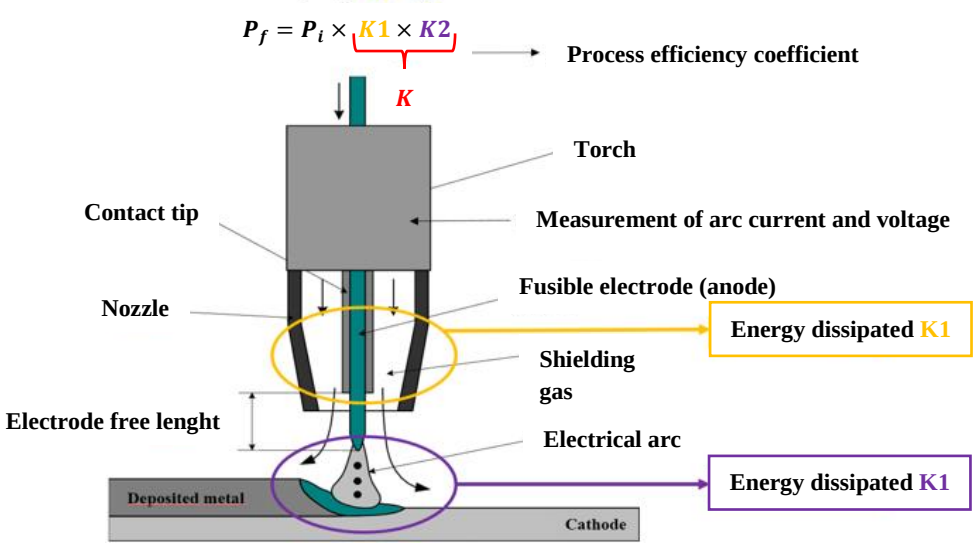

Figure 9: Phenomena of energy losses of the WAAM process (CMT and CMT +P)

The coefficient "K" was calibrated by comparison of the bead's dimensional criterion of the simulated and experimentally obtained bead. The method included analyzing the width and hight of both samples. The input parameters are presented (Table 3). The transmitted arc power, denoted as "P_f", can be calculated using the (Eq 2).

$$K = K1 * K2 \ (1)$$

$$P_f = P_i \times K \ (2)$$

Table 3 : Input parameters to sample 1

Parameters	WFS (m/min)	TS (mm/min)	Wire Ø (mm)	Shield gas	P(W)	K
Experiment	7.6	320	1.2	50% Ar +He	2000	/
Simulation	7.6	320	1.2	50% Ar +He	2000	0.64

The (Figure 10) demonstrated different simulation tests carried out to calibrate "*K*". Considering previously set geometric criterion and the shape of the simulated and experimental bead, the coefficient value was set to constant of 0.64.

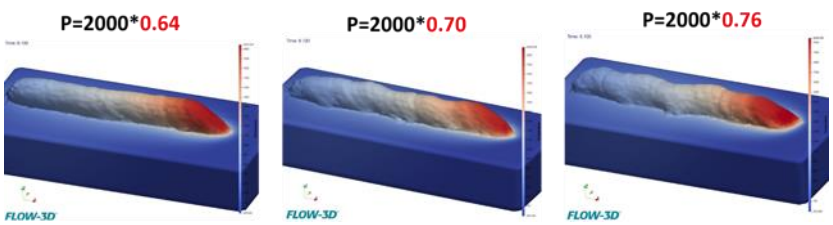

Figure 10: Calibration of K coefficient

Maintaining this parameter is crucial given it is role as a factor in the energy input during the process. Consequently, it exerts a strong influence on the geometry of beads and walls.

4 RESULTS AND DISCUSSIONS

4.1 Simulation results

A variation of parameters is applied to assess the correlation with experimental results. Simulations were conducted for Sample 1 (CMT) and 5 (CMT+P) using the parameters obtained from previous calibration studies, as listed in (Table 4).

Table 4 : Input setup to simulated trial with CMT (sample 1) and CMT+P (sample 5)

N°	P (W)	Coefficient rate	TS (mm/min)	WFS (m/min)
1	2000	0.64	320	8
5	3500	0.64	320	6

The results illustrate that data from numerical and experimental model are aligned. For instance, (Figure 11) demonstrates results of the process parametric set up N°1 (data from table 4) showing 5% difference of the bead width.

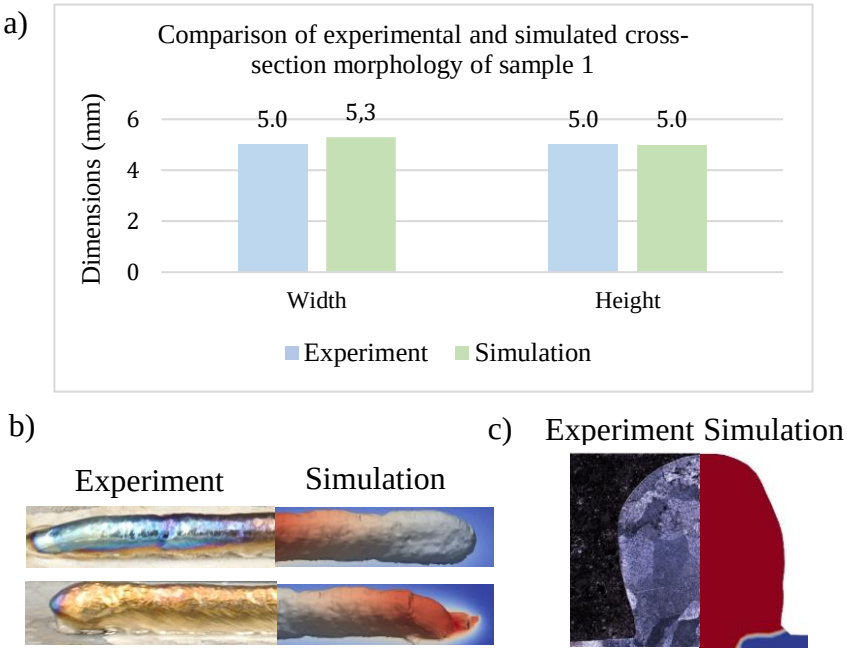

Figure 11: Sample 1, CMT. a) Dimensions comparison. b) 3D comparison. c) Comparison of 2D transverse section.

Additionally, in (Figure 12), represents similar findings for another set of parameters (N°5, table 4). Here, only 5% error is observed for both height and width. Thus, these results confirm the model's reability.

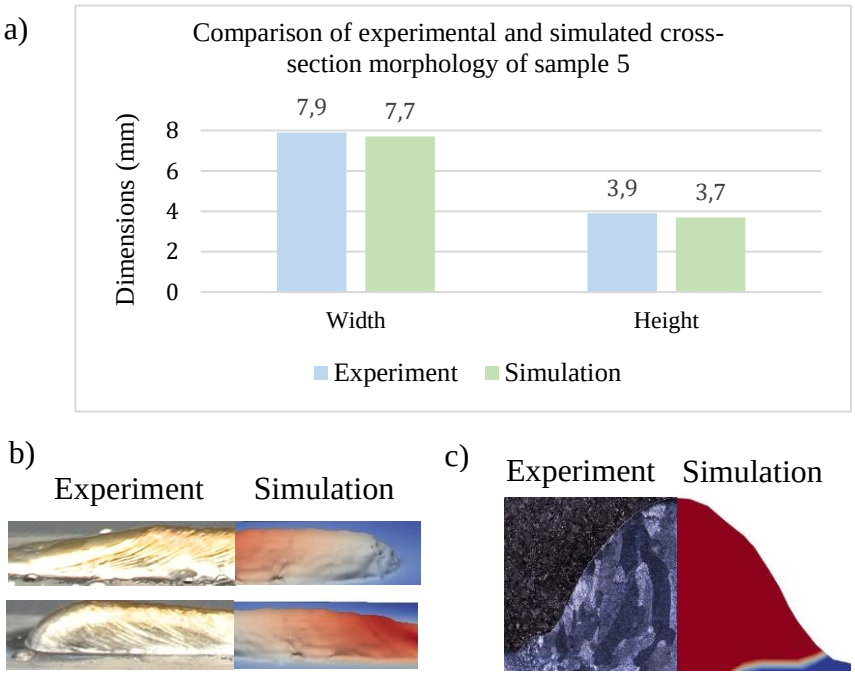

Figure 12: Sample 5, CMT+P. a) Dimensions comparison. b) 3D comparison. c) Comparison of 2D transverse section.

To further prove the method's efficienty, the modelling set up was applied for muli-layered wall. Once again, the results were evaluated based on the weight and height criterion. The multi-layered wall was fabricated in back-and-forth manner with CMT process. Initially, visual comparsion showed consistency between the experiments and the simulation. Additionally, (Figure 13) demonstrates that the thermo-fluid model was able to predict the topology of the wall through edged distinction of the start and end points.

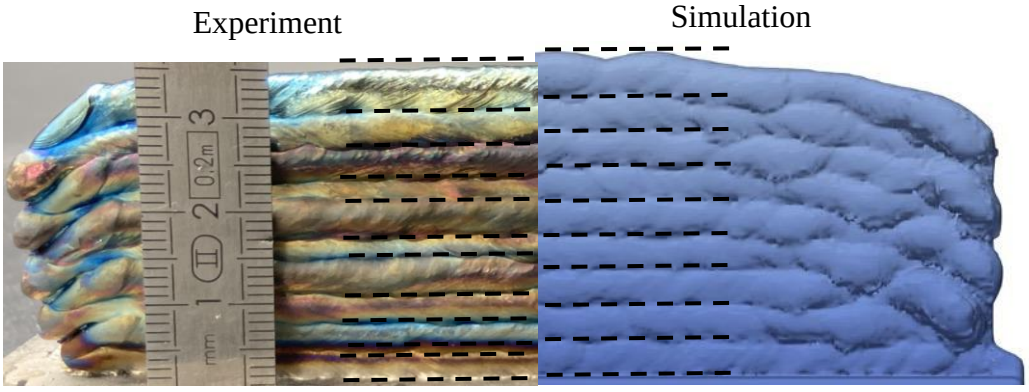

Figure 13: Comparison of 10 layers wall for experiment and 9 layers for simulated results

(Figure 14) illustrates the evaluated samples reveling 3% and 22% error between the experimental and numerical bead's width and height respectively. These findings demonstrate that while the model is capable to precisely predict the width, it is less accurate for estimating the height. Therefore, it was postulated that reason for this phenomenon can be attributed to the error accumulation. These errors accumulations are caused by the differences between the idle time of the numerical and experimental model,

effecting the thermal history. Further experiments and simulations need to be conducted to obtain more reliable results.

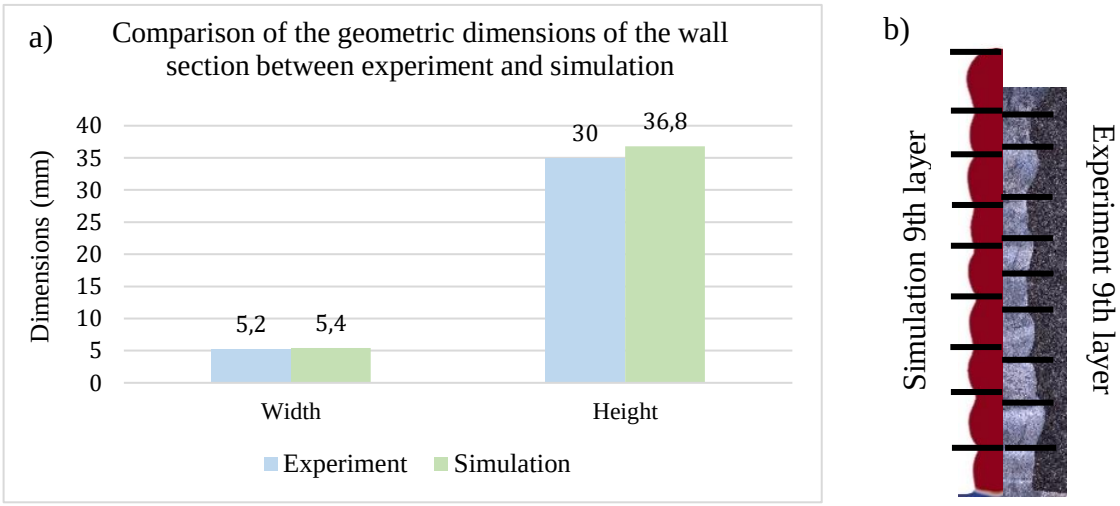

Figure 14: Wall, CMT, a) Dimensions comparison, b) Comparison of 2D transverse section

In conclusion, the model proves valuable for predicting the geometry of individual deposited layers and multiple layers produced using the WAAM process. Leveraging experimental power signals from the CMT transfer mode enhances our understanding of the electric arc's underlying physics. The model offers an initial insight into the geometry of beads and the surface topology of walls. In addition, the thermo-fluid model demonstrates the capability to predict thermal history. However, certain assumptions, such as neglecting the effects of Lorentz forces, wire retraction dynamics and droplets transfer were not employed. The latter assumption diminishes the transfer metal's impact on the melt pool itself and reduces its penetration, influencing the melt's geometry and, consequently, the deposited beads. As a result, some dimensional differences between simulation and experimental outcomes are observed, particularly accentuated in multilayer depositions due to cumulative modelling errors.

5 Conclusion

A mesoscale 3D thermo-fluid model of the WAAM process utilizing CMT has been developed. The model captured bead deposition at alterning parameters for both CMT and CMT+P. Additionally, a ten-layer wall was fabricated using CMT. The simulation examined key elements, including the wire-substrate motion, material flow, CMT technology energy input, metal vaporization, melt processes, phase transitions, and fluid dynamics Ti-6Al-4V material properties. This work marks four significant contributions, presented in the following:

(1) The thermo-fluid model can accurately predict the geometry of one bead and walls with CMT technologies as a function of the Ti-6Al-4V properties.
(2) The model elucidates the impact of travel speed, wire feed speed and energy input parameters on the bead geometry.
(3) The model provides a distinction between CMT and CMT+P.

(4) The suggested thermo-fluid model can be extended for computing thermal data to be incorporated into micro and macro scale models in future research endeavours.

References

Bai, X., Colegrove, P., Ding, J., Zhou, X., Diao, C., Bridgeman, P., roman Hönnige, J., Zhang, H., & Williams, S. (2018). Numerical analysis of heat transfer and fluid flow in multilayer deposition of PAW-based wire and arc additive manufacturing. International Journal of Heat and Mass Transfer, 124, 504–516.

Benoit, A. (2018). Développement du soudage MIG CMT pour la réparation de pièces aéronautiques. Application auxpièces en alliage base aluminium 6061. HAL Id: tel-01674156.

Cadiou, S.,. (2020). Fabrication additive arc-fil (WAAM) To cite this version : HAL Id : tel-02496906

Cheon, J., Kiran, D. V., & Na, S. J. (2016). CFD based visualization of the finger shaped evolution in the gas metal arc welding process. International Journal of Heat and Mass Transfer, 97, 1–14.

Fronius, "Fronius RCU 5000 Operating Manual",n.d, (2021).

≪ Fronius, Cold Metal Transfer : The technology, CMT technology ≫, www.fronius.com, 2023.

Gokhale, N. P., & Kala, P. (2021). Thermal analysis of TIG-WAAM based metal deposition process using finite element method. Materials Today: Proceedings, 44, 453–459.

Hamid Heza Saedi. (1989). Thermal-Fluid Model for Weld Pool Geometry Dynamics. Unkel, W.

Hascoet, J.-Y., Pechet, G., Rauch, M., Ruckert, G., 2018. Study of the impact of the heat input for NAB parts manufactured in WAAM, in: Manufacturing Conference. Paris (France).

Justus Panicker, C. T., Rohit Surya, K., & Senthilkumar, V. (2022). Novel process parameters based approach for reducing residual stresses in WAAM. Materials Today: Proceedings.

J. Goldak, A. Chakravarti, and M. Bibby, "A new finite element model for welding heat sources," Metall. Trans. B, 1984.

Montevecchi, F., Venturini, G., Scippa, A., & Campatelli, G. (2016). Finite Element Modelling of Wire-arc-additive-manufacturing Process. Procedia CIRP, 55, 109–114.

Nezamdost, M. R., Esfahani, M. R. N., Hashemi, S. H., & Mirbozorgi, S. A. (2016). Investigation of temperature and residual stresses field of submerged arc welding by finite element method and experiments. International Journal of Advanced Manufacturing Technology, 87(1–4), 615–624.

Ogino, Y. et Hirata, Y. (2015). Numerical simulation of metal transfer in argon gas-shielded GMAW. Welding in the World, 59(4):465–473.

Panwisawas, C., Sovani, Y., Turner, R. P., Brooks, J. W., Basoalto, H. C., & Choquet, I. (2018). Modelling of thermal fluid dynamics for fusion welding. Journal of Materials Processing Technology, 252, 176–182.

Prado-Cerqueira, J. L., Diéguez, J. L., & Camacho, A. M. (2017). Preliminary development of a Wire and Arc Additive Manufacturing system (WAAM). Procedia Manufacturing, 13, 895–902.

Rauch, M., Nwankpa, V. U., Pechet, G., & Rückert, G. (2022). A methodology for large parts Wire and Arc Additive Manufacturing- A ship propeller blade as case study. American Journal of Engineering, Science and Technology (AJEST) 14, 32–41.

Rauch, M., Pechet, G., Hascoet, J.Y., Ruckert, G., 2021. Extending High Value Components Performances with Additive Manufacturing: Application to Naval Applications. Solid State Phenom.

Rauch, M., Dorado, J. P., Hascoet, J.-Y., & Ruckert, G. (2021). A novel method for additive manufacturing of complex shape curved parts by using variable height layers. Journal of Machine Engineering, 21(3), 80--91.

Sampaio, R. F. V., Pragana, J. P. M., Bragança, I. M. F., Silva, C. M. A., Nielsen, C. V., & Martins, P. A. F. (2023). Modelling of wire-arc additive manufacturing – A review. Advances in Industrial and Manufacturing Engineering, 6, 100121.

Shah, A., Aliyev, R., Zeidler, H., & Krinke, S. (2023). A Review of the Recent Developments and Challenges in Wire Arc Additive Manufacturing (WAAM) Process. Journal of Manufacturing and Materials Processing, 7(3), 97.

Srinivasan, D., Sevvel, P., Solomon, I. J., & Tanushkumaar, P. (2022). A review on Cold Metal Transfer (CMT) technology of welding Selection and peer-review under responsibility of the scientific committee of the International Conference on Advanced Materials for Innovation and Sustainability.2022.04.016

Singh, S., kumar Sharma, S., & Rathod, D. W. (2021). A review on process planning strategies and challenges of WAAM. Materials Today: Proceedings 47, 6564–6575656.

Wu, B., Pan, Z., Ding, D., Cuiuri, D., Li, H., Xu, J., & Norrish, J. (2018). A review of the wire arc additive manufacturing of metals: properties, defects and quality improvement. Journal of Manufacturing Processes, 35(July), 127–139.

Xin, H., Tarus, I., Cheng, L., Veljkovic, M., Persem, N., & Lorich, L. (2021). Experiments and numerical simulation of wire and arc additive manufactured steel materials. Structures, 34, 1393–1402.

Zhao, W., Tashiro, S., Murphy, A. B., Tanaka, M., Liu, X., & Wei, Y. (2023). Deepening the understanding of arc characteristics and metal properties in GMAW-based WAAM with wire retraction via a multi-physics model. Journal of Manufacturing Processes, 97(May), 260–274.